6th European Conference on Computational Mechanics (ECCM 6)
7th European Conference on Computational Fluid Dynamics (ECFD 7)
11 – 15 June 2018, Glasgow, UK

GENERAL BOUNDARY ELEMENT METHOD FOR DUAL-PHASE LAG EQUATION

E. MAJCHRZAK

Silesian University of Technology
44-100 Gliwice, Konarskiego 18a, Poland
Ewa.Majchrzak@polsl.pl

Key words: Dual-Phase Lag Equation, Numerical Methods, General Boundary Element Method.

1 INTRODUCTION

Dual-phase lag equation (DPLE) is used, among others, for the description of heat transfer processes proceeding in the micro scale [1-4], e.g. for determining the temperature distribution in the thin metal film subjected to an ultra-short laser pulse. In the problems of this type, because of the extremely short duration, the extreme temperature gradients and the very small thickness of the film domain, the finite velocity of the thermal wave must be considered. The DPLE is also used for the numerical modeling of thermal phenomena occurring in the biological tissue heated by the external heat sources, e.g. [5-9]. In this case the DPL model describes a macroscopic temperature wherein an inner microscopic tissue structure is taken into account. In the paper the one dimensional problems are considered because the layer of the thin metal film and the layer of skin tissue can be treated as the 1D objects. Dual-phase lag equation contains a second order time derivative and higher order mixed derivative in both time and space. Two positive constants, it means the thermalization time and relaxation time appear in this equation. So far, the dual-phase lag equation supplemented by appropriate boundary and initial conditions is most often solved using the finite difference method in its various variants (explicit and implicit schemes, e.g. [10-13], generalized finite difference method [14]). In this work, the approach based on the concept of the boundary element techniques [15, 16] is proposed. It should be noted that for the DPLE the corresponding fundamental solution is either unknown or very difficult to obtain. But, using the homotopy analysis method, introduced first by Liao [17-19], it is possible to elaborate the general boundary element method for the equation considered. At the first stage, for the purpose of numerical stability, the DPL equation is discretized in the time domain in terms of a fully implicit form with the backward finite-difference method for both first- and second-order time derivatives. In this way one obtains the equations that present a non-linear boundary-value problem at the each time step. Next, the non-linear and linear differential operators are defined [17, 18, 20, 21]. The equation associated with the first-order deformation derivative resulting from the homotopy analysis method can be solved using the traditional boundary element method for steady state problem [15, 16]. In the paper [22] the other variant of the BEM, in particular the boundary element method using discretization in time (e.g. [23]) has been applied for the solution of the similar problems, but the algorithm presented here is more exact and more effective (especially at the stage of the space-time grid selection).

2 DUAL-PHASE LAG EQUATION

The 1D dual-phase lag equation has the following form [1-4]

$$c\frac{\partial T(x,t)}{\partial t}+c\,\tau_q\frac{\partial^2 T(x,t)}{\partial t^2}=\lambda\frac{\partial^2 T(x,t)}{\partial x^2}+\lambda\tau_T\frac{\partial^3 T(x,t)}{\partial t\partial x^2}+S(x,t)+\tau_q\frac{\partial S(x,t)}{\partial t} \tag{1}$$

where c is a volumetric specific heat of material, λ is a thermal conductivity, τ_q and τ_T are the phase lags (relaxation and thermalization times), S is the capacity of internal heat sources, T, x, t denote the temperature, geometrical co-ordinate and time.

The equation (1) is supplemented by the modified Neumann boundary conditions for $x = 0$ and $x = L$

$$q_b(x,t)+\tau_q\frac{\partial q_b(x,t)}{\partial t}=-\lambda\left[\frac{\partial T(x,t)}{\partial x}+\tau_T\frac{\partial}{\partial t}\left(\frac{\partial T(x,t)}{\partial x}\right)\right] \tag{2}$$

where $q_b(x, t)$ is the boundary heat flux.

The initial conditions are also given

$$t=0:\quad T(x,0)=T_p(x),\quad \left.\frac{\partial T(x,t)}{\partial t}\right|_{t=0}=w(x) \tag{3}$$

where $T_p(x)$ is the initial temperature, $w(x)$ is the initial heating rate.

Dual-phase lag equation is used, among others, for numerical modeling of thermal processes occurring in the thin metal film subjected to the laser pulse [13, 24, 25]. As mentioned, the dominant direction of heat transfer is the direction perpendicular to the layer and therefore the 1D model can be considered. The laser irradiation is described by the following internal source term (equation (1))

$$S(x,t)=\sqrt{\frac{\beta}{\pi}}\frac{1-R}{t_p\,\delta}\,I_0\,\exp\left[-\frac{x}{\delta}-\beta\frac{(t-2t_p)^2}{t_p^2}\right] \tag{4}$$

where I_0 is the laser intensity, t_p is the characteristic time of laser pulse, δ is the optical penetration depth, R is the reflectivity of the irradiated surface and $\beta = 4\ln 2$ [25].

The DPLE is also used in numerical modeling of thermal phenomena occurring in living organisms subjected to the strong external heat sources. Blood perfusion and metabolic processes occurring in the living tissues are taken into account as the components of the source term $S(x, t)$ (c.f. equation (1)), namely

$$S(x,t)=w_B c_B[T_B-T(x,t)]+Q_m \tag{5}$$

where w_B [kg/(m^3 s)] is the blood perfusion rate, c_B is the specific heat of blood, T_B is the arterial blood temperature and Q_m is the metabolic heat source.

Introducing (5) into equation (1) one has

$$\begin{aligned}&\left(c+\tau_q w_B c_B\right)\frac{\partial T(x,t)}{\partial t}+c\,\tau_q\frac{\partial^2 T(x,t)}{\partial t^2}=\\&\lambda\frac{\partial^2 T(x,t)}{\partial x^2}+\lambda\tau_T\frac{\partial^3 T(x,t)}{\partial t\partial x^2}-w_B c_B T(x,t)+w_B c_B T_B+Q_m\end{aligned}\tag{6}$$

The equations (1) and (6) can be written in the form

$$\begin{aligned}&\left(c+s\tau_q w_B c_B\right)\frac{\partial T(x,t)}{\partial t}+c\,\tau_q\frac{\partial^2 T(x,t)}{\partial t^2}=\\&\lambda\frac{\partial^2 T(x,t)}{\partial x^2}+\lambda\tau_T\frac{\partial^3 T(x,t)}{\partial t\partial x^2}-s w_B c_B T(x,t)+Q(x,t)\end{aligned}\tag{7}$$

where s=0 corresponds to the equation (1), s=1 is related to the bioheat transfer equation (6), while

$$Q(x,t):\begin{cases}S(x,t)+\tau_q\dfrac{\partial S(x,t)}{\partial t}, & s=0\\ w_B c_B T_B+Q_m, & s=1\end{cases}\tag{8}$$

3 GENERAL BOUNDARY ELEMENT METHOD

At the first stage, for the purpose of numerical stability, the DPL equation (7) is discretized in the time domain in terms of a fully implicit form with the backward finite-difference method for both the first- and second-order time derivatives

$$\begin{aligned}&\left(c+s\tau_q w_B c_B\right)\frac{T^f(x)-T^{f-1}(x)}{\Delta t}+c\,\tau_q\frac{T^f(x)-2T^{f-1}(x)+T^{f-2}(x)}{\left(\Delta t\right)^2}=\\&\lambda\frac{\partial^2 T^f(x)}{\partial x^2}+\frac{\lambda\tau_T}{\Delta t}\left[\frac{\partial^2 T^f(x)}{\partial x^2}-\frac{\partial^2 T^{f-1}(x)}{\partial x^2}\right]-s w_B c_B T^f(x)+Q^f(x)\end{aligned}\tag{9}$$

where $T^f(x)=T(x, f\Delta t)$, Δt is the time step, f=2, 3, ..., F and $T^{f-1}(x)$, $T^{f-2}(x)$ are known temperature distributions at (f–1)th and (f–2)th time steps, respectively. It should be noted that taking into account the initial conditions (3) one has: $T^0(x)= T_0$, $T^1(x)= T_0+ w(x)\Delta t$.

The boundary conditions (2) are also transformed

$$q_b^f(x)+\tau_q\left(\frac{\partial q_b(x,t)}{\partial t}\right)^f=-\lambda\left[\frac{\partial T^f(x)}{\partial x}+\frac{\tau_T}{\Delta t}\left(\frac{\partial T^f(x)}{\partial x}-\frac{\partial T^{f-1}(x)}{\partial x}\right)\right]\tag{10}$$

In this way one obtains the equations that present a boundary-value problem at each time step.

The equations (9), (10) can be written in the form

$$\frac{\partial^2 T^f(x)}{\partial x^2}-BT^f(x)+C\frac{\partial^2 T^{f-1}(x)}{\partial x^2}+DT^{f-1}(x)+ET^{f-2}(x)+FQ^f(x)=0\tag{11}$$

and

$$-\lambda\frac{\partial T^f(x)}{\partial x}=w_b^f(x) \tag{12}$$

where

$$\begin{aligned}
&B=\frac{\left(c+s\,w_B c_B\Delta t\right)(\Delta t+\tau_q)}{\lambda\Delta t(\Delta t+\tau_T)},\quad C=-\frac{\tau_T}{\Delta t+\tau_T}\\
&D=\frac{c(\Delta t+2\tau_q)+s\,\tau_q w_B c_B\Delta t}{\lambda\Delta t(\Delta t+\tau_T)}\\
&E=-\frac{c\,\tau_q}{\lambda\Delta t(\Delta t+\tau_T)},\quad F=\frac{\Delta t}{\lambda(\Delta t+\tau_T)}
\end{aligned} \tag{13}$$

while

$$w_b^f(x)=\frac{\Delta t}{\Delta t+\tau_T}\left[q_b^f(x)+\tau_q\left(\frac{\partial q_b(x,t)}{\partial t}\right)^f\right]-\frac{\lambda\tau_T}{\Delta t+\tau_T}\frac{\partial T^{f-1}(x)}{\partial x} \tag{14}$$

Using the homotopy analysis method [17, 18, 20, 21], the equation (11) can be represented as

$$\begin{aligned}
&\frac{\partial^2 U^{[1]}(x)}{\partial x^2}-BU^{[1]}(x)+\frac{\partial^2 U(x)}{\partial x^2}-BU(x)+C\frac{\partial^2 T^{f-1}(x)}{\partial x^2}+DT^{f-1}(x)+\\
&ET^{f-2}(x)+FQ^f(x)=0
\end{aligned} \tag{15}$$

where

$$U^{[1]}(x)=\left.\frac{\partial\,\Phi(x;p)}{\partial\,p}\right|_{p=0} \tag{16}$$

while $\Phi(x;\,p)$ is the function (homotopy) associated with the family of partial differential equations [17, 18], $p\in[0,\,1]$ is the embedding parameter and $U(x)$ is an initial approximation of temperature distribution $T^f(x)$ (e.g. $U(x)=T^{f-1}(x)$).

The equation (15) is supplemented by boundary conditions [17]

$$-\lambda\frac{\partial U^{[1]}(x)}{\partial x}=w_b^f(x)+\lambda\frac{\partial U(x)}{\partial x} \tag{17}$$

After solving the problem (15), (17), the temperature distribution $T^f(x)$ is calculated using the formula

$$T^f(x)=U(x)+U^{[1]}(x) \tag{18}$$

The equation (15) can be written in the form

$$\frac{\partial^2 U^{[1]}(x)}{\partial x^2} - BU^{[1]}(x) + R\left[U(x)\right] = 0 \tag{19}$$

where

$$R\left[U(x)\right] = \frac{\partial^2 U(x)}{\partial x^2} - BU(x) + C\frac{\partial^2 T^{f-1}(x)}{\partial x^2} + DT^{f-1}(x) + ET^{f-2}(x) + FQ^{f}(x) \tag{20}$$

To solve the equation (19) the weighted residual method criterion is used [15, 16]

$$\int_0^L \left[\frac{\partial^2 U^{[1]}(x)}{\partial x^2} - BU^{[1]}(x) + R\left[U(x)\right] \right] T^*(\xi, x)\,\mathrm{d}x = 0 \tag{21}$$

where $\xi \in (0, L)$ is the observation point, while $T^*(\xi, x)$ is the fundamental solution and for the 1D objects oriented in rectangular co-ordinate system it is a function of the form [15]

$$T^*(\xi,\ x) = \frac{1}{2\sqrt{B}}\ \exp\left(-\left|x-\xi\right|\sqrt{B}\right) \tag{22}$$

One can check that the fundamental solution fulfils the equation

$$\frac{\partial^2 T^*(\xi, x)}{\partial x^2} - BT^*(\xi, x) = -\delta(\xi, x) \tag{23}$$

where $\delta(\xi, x)$ is the Dirac function.

The formula determining the heat flux resulting from the fundamental solution $q^*(\xi, x) = -\lambda\, \partial T^*(\xi, x) / \partial x$ can be calculated in analytical way, namely

$$q^*(\xi, x) = \frac{\lambda\,\mathrm{sgn}(x-\xi)}{2}\ \exp\left(-\left|x-\xi\right|\ \sqrt{B}\ \right) \tag{24}$$

where sgn(·) is the sign function.

Integrating twice by parts the first component of equation (21) and taking into account the property of fundamental solution (23), one obtains

$$U^{[1]}(\xi) + \frac{1}{\lambda}\left[T^*(\xi, x) W^{[1]}(x)\right]_{x=0}^{x=L} = \frac{1}{\lambda}\left[q^*(\xi, x) U^{[1]}(x)\right]_{x=0}^{x=L} + Z(\xi) \tag{25}$$

where

$$Z(\xi) = \int_0^L R\left[U(x)\right]\ T^*(\xi, x)\,\mathrm{d}x \tag{26}$$

and $W^{[1]}(x) = -\lambda\, \partial\, U^{[1]}(x) / \partial x$.

To calculate the integral $Z(\xi)$, the domain $[0, L]$ is divided into n constant internal cells ($h=L/n$ is the length of internal cell), the nodes 0 and $n+1$ are located on the boundaries $x = 0$ and $x = L$, respectively, while $x_i = ih - h/2$, $i = 1, 2, ..., n$ are the internal nodes. The integral (26)

is substituted by the sum of integrals from x_i–h/2 to x_i +h/2. These integrals are calculated using the 6-points Gauss quadratures.

The method of approximation of second order derivatives of functions $U(x)$ and $T^{f-1}(x)$ with respect to x should be explained (formula (20)). In the case of constant internal cells one has

$$\begin{aligned}
\left[\frac{\partial^2 U(x)}{\partial x^2}\right]_1 &= \frac{8U_0 - 12U_1 + 4U_2}{3h^2} \\
\left[\frac{\partial^2 U(x)}{\partial x^2}\right]_i &= \frac{U_{i-1} - 2U_i + U_{i+1}}{h^2}, \quad i = 2,3,...,n-1 \\
\left[\frac{\partial^2 U(x)}{\partial x^2}\right]_n &= \frac{4U_{n-1} - 12U_n + 8U_{n+1}}{3h^2}
\end{aligned} \tag{27}$$

and

$$\begin{aligned}
\left[\frac{\partial^2 T^{f-1}(x)}{\partial x^2}\right]_1 &= \frac{8T_0^{f-1} - 12T_1^{f-1} + 4T_2^{f-1}}{3h^2} \\
\left[\frac{\partial^2 T^{f-1}(x)}{\partial x^2}\right]_i &= \frac{T_{i-1}^{f-1} - 2T_i^{f-1} + T_{i+1}^{f-1}}{h^2}, \quad i = 2,3,...,n-1 \\
\left[\frac{\partial^2 T^{f-1}(x)}{\partial x^2}\right]_n &= \frac{4T_{n-1}^{f-1} - 12T_n^{f-1} + 8T_{n+1}^{f-1}}{3h^2}
\end{aligned} \tag{28}$$

For $\xi \to 0^+$ and $\xi \to L^-$ one obtains the equations which can be written in the matrix form

$$\begin{bmatrix} -\frac{1}{2\lambda\sqrt{B}} & \frac{1}{2\lambda\sqrt{B}}\exp\left(-L\sqrt{B}\right) \\ -\frac{1}{2\lambda\sqrt{B}}\exp\left(-L\sqrt{B}\right) & \frac{1}{2\lambda\sqrt{B}} \end{bmatrix} \begin{bmatrix} W^{[1]}(0) \\ W^{[1]}(L) \end{bmatrix} = \begin{bmatrix} -\frac{1}{2} & \frac{1}{2}\exp\left(-L\sqrt{B}\right) \\ \frac{1}{2}\exp\left(-L\sqrt{B}\right) & -\frac{1}{2} \end{bmatrix} \begin{bmatrix} U^{[1]}(0) \\ U^{[1]}(L) \end{bmatrix} + \begin{bmatrix} Z(0) \\ Z(L) \end{bmatrix} \tag{29}$$

where (c.f. equations (14), (17))

$$W^{[1]}(x) = -\lambda\frac{\partial U^{[1]}(x)}{\partial x} = \frac{\Delta t}{\Delta t + \tau_T}\left[q_b^f(x) + \tau_q\left(\frac{\partial q_b(x,t)}{\partial t}\right)^f\right] - \frac{\lambda\tau_T}{\Delta t + \tau_T}\frac{\partial T^{f-1}(x)}{\partial x} + \lambda\frac{\partial U(x)}{\partial x} \tag{30}$$

Using the dependence (30) the following approximation is introduced

$$W^{[1]}(0)=\frac{\Delta t}{\Delta t+\tau_T}\left[q_b^f(0)+\tau_q\left(\frac{\partial q_b(0,t)}{\partial t}\right)^f\right]-\frac{\lambda\tau_T}{\Delta t+\tau_T}\frac{T_1^{f-1}-T_0^{f-1}}{h/2}+\lambda\frac{U_1-U_0}{h/2} \tag{31}$$

$$W^{[1]}(L)=\frac{\Delta t}{\Delta t+\tau_T}\left[q_b^f(L)+\tau_q\left(\frac{\partial q_b(L,t)}{\partial t}\right)^f\right]-\frac{\lambda\tau_T}{\Delta t+\tau_T}\frac{T_{n+1}^{f-1}-T_n^{f-1}}{h/2}+\lambda\frac{U_{n+1}-U_n}{h/2} \tag{32}$$

and then, from the system of equations (29), the boundary values $U^{[1]}(0)$, $U^{[1]}(L)$ are determined.

Next, the values of function $U^{[1]}(x)$ at the internal points x_i, i=1, 2, ..., n are calculated (c.f. equation (25))

$$\begin{aligned}U_i^{[1]}=&\frac{1}{2}\exp\left[-(L-x_i)\sqrt{B}\right]U^{[1]}(L)+\frac{1}{2}\exp\left[-x_i\sqrt{B}\right]U^{[1]}(0)-\\&\frac{1}{2\lambda\sqrt{B}}\exp\left[-(L-x_i)\sqrt{B}\right]W^{[1]}(L)+\frac{1}{2\lambda\sqrt{B}}\exp\left[-x_i\sqrt{B}\right]W^{[1]}(0)+Z(x_i)\end{aligned} \tag{33}$$

Finally, the temperature distribution in all nodes is determined using the formula (18). The obtained temperature field constitutes the pseudo-initial condition for the next loop of computations.

4 RESULTS OF COMPUTATIONS

To test the accuracy and effectiveness of the method proposed, at first the following task has been solved. A layer of thickness $L=10^{-4}$ with thermophysical parameters equal $\lambda = 1$, $c = 1$, $\tau_q = 1/\pi^2 + 100$, $\tau_T = 1/\pi^2 + 10^{-6}$ is considered. Thus, the following equation is taken into account

$$\frac{\partial T(x,t)}{\partial t}+\left(\frac{1}{\pi^2}+100\right)\frac{\partial^2 T(x,t)}{\partial t^2}=\frac{\partial^2 T(x,t)}{\partial x^2}+\left(\frac{1}{\pi^2}+10^{-6}\right)\frac{\partial^3 T(x,t)}{\partial t\,\partial x^2} \tag{34}$$

with the boundary and initial conditions

$$T(0,t)=0,\qquad T(G,t)=0 \tag{35}$$

$$T(x,0)=\sin(10^4\pi x),\qquad \left.\frac{\partial T(x,t)}{\partial t}\right|_{t=0}=-\pi^2\sin(10^4\pi x) \tag{36}$$

Analytical solution of the problem formulated above is the following [26]

$$T(x,t)=\exp(-\pi^2 t)\ \sin(10^4\pi x) \tag{37}$$

In Figure 1 the comparison of analytical and numerical solutions for different moments of time is shown. The computations using general boundary element method have been done for time step Δt = 0.005 and n = 100 internal cells. A very good agreement between both solutions is visible.

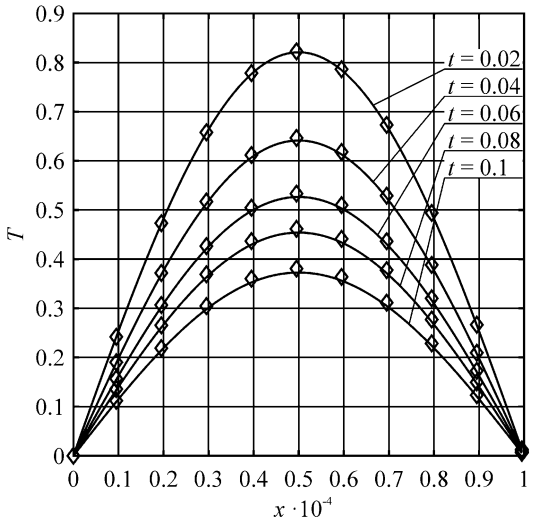

Figure 1: Analytical (lines) and numerical (symbols) solutions

Let us define the error of numerical solution as follows

$$Err = \sqrt{\frac{1}{F(n+2)} \sum_{f=1}^{F} \sum_{i=0}^{n+1} \left(T_i^f - T_{ai}^f \right)^2} \tag{38}$$

where F is the number of time steps, while T_{ai}^f are the local and temporary temperatures resulting from the analytical solution. The testing computations concerning the values of Err for different discretizations of time and space are collected in table 1.

Table 1: Error for different time steps and number of internal cells.

Δt	$n = 50$	$n = 100$	$n = 200$	$n = 1000$
0.0005	$5.753 \cdot 10^{-4}$	$5.074 \cdot 10^{-4}$	$4.904 \cdot 10^{-4}$	$4.855 \cdot 10^{-4}$
0.001	$1.035 \cdot 10^{-4}$	$9.705 \cdot 10^{-4}$	$9.548 \cdot 10^{-4}$	$9.508 \cdot 10^{-4}$
0.005	$41.013 \cdot 10^{-4}$	$40.058 \cdot 10^{-4}$	$40.476 \cdot 10^{-4}$	$40.501 \cdot 10^{-4}$
0.01	$68.761 \cdot 10^{-4}$	$68.544 \cdot 10^{-4}$	$68.457 \cdot 10^{-4}$	$68.539 \cdot 10^{-4}$
0.015	$78.272 \cdot 10^{-4}$	$78.080 \cdot 10^{-4}$	$78.125 \cdot 10^{-4}$	$78.232 \cdot 10^{-4}$

As can be seen, for all variants of computations the errors are quite small. A greater impact on the error has a time step Δt than the number of internal cells n. In contrast to the BEM using discretization in time [22], in the case of GBEM application, the selection of the proper time step and the number of internal cells is not difficult, because they can change in a quite wide range.

Next, the general boundary element method is used in order to determine the temperature field in the thin metal film subjected to the laser pulse [13, 24, 25]. As an example, the gold layer with thickness $L = 100$ nm is considered. The layer is subjected to a short-pulse laser irradiation ($R = 0.93$, $I_0 = 13.7$ J/m^2, $t_p = 0.1$ ps, $\delta = 15.4$ nm). Thermophysical parameters of material are the following: $\lambda = 317$ W/(mK), $c = 2.4897$ MJ/(m^{3}K), $\tau_q = 8.5$ ps, $\tau_T = 90$ ps [13]. For $x = 0$ and $x = L$ the non-flux conditions should be assumed (in equation (2): $q_b(x, t)=0$). The initial

temperature is equal to 300 K, initial heating rate $w(x)=0$ (c.f. equation (3)). The number of internal cells $n = 100$, time step $\Delta t = 0.01$ ps.

In Figure 2 the temperature history at the point $x=0$ corresponding to the irradiated surface is shown. In this Figure the solution related to the macroscopic Fourier equation ($\tau_q = 0$, $\tau_T = 0$) is also presented. As can be seen, the differences are significant, the Fourier model overestimates the temperature values, which is also demonstrated in experimental studies [27, 28].

It should be noted that the problem formulated above, has been solved using implicit scheme of the finite difference method [29] and the results are practically the same, which confirms the correctness of the GBEM algorithm.

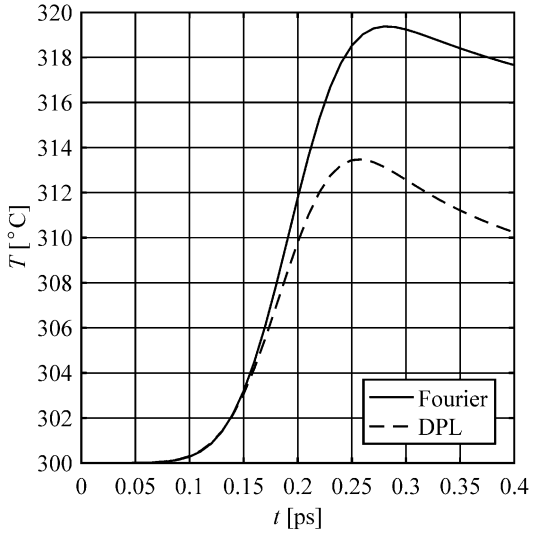

Figure 2: Temperature history at the irradiated surface of thin gold film

The next application area of the dual-phase lag equation is the modeling of thermal processes taking place in the heated or cooled living tissues [5-9, 30-33]. As an example, the skin layer of thickness $L = 0.03$ m subjected to the external heat flux q_b=1000 W/m^2 (c.f. equation (2) for $x=0$) is considered. For $x=L$ the Neumann condition $q_b(x, t)=0$ is assumed. The initial temperature equals 37^{0}C, while the initial heating rate $w(x)$ is equal to 0 (c.f. equation (3)).

The following values of parameters are assumed: volumetric specific heat of tissue $c = 4 \cdot 10^6$ W/(m^3 K), thermal conductivity of tissue $\lambda = 0.5$ W/(m K), blood perfusion rate $w_B = 0.53$ kg/(m^3 s), specific heat of blood $c_B = 3\,770$ W/(kg K), blood temperature $T_B = 37$ ºC, metabolic heat source $Q_m = 245$ W/m^3, relaxation time $\tau_q = 15$ s, thermalization time $\tau_T = 10$ s [30].

In Figure 3 the temperature distribution for $x \leq 0.01$m is presented. As it is visible, after 90 seconds, only the layer with the thickness of 1 mm has reached the temperature above 42^{0}C (such a temperature can cause the burns). Figure 4 illustrates the curves at the heated surface $x=0$ both for the DPL equation and the Fourier model ($\tau_q = 0$, $\tau_T = 0$). The temperatures obtained using the DPLE are lower in comparison with the Fourier model because the parameters τ_q and τ_T take into account the phase-lag in establishing heat flux (relaxation time τ_q) and phase-lag in establishing the temperature gradient (thermalization time τ_q).

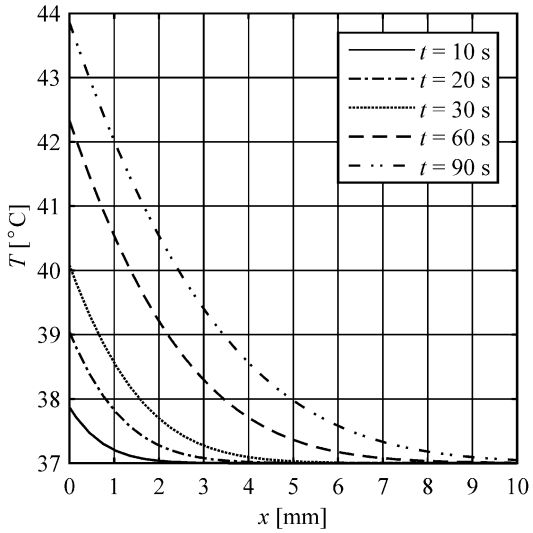

Figure 3: Temperature distribution in the heated tissue

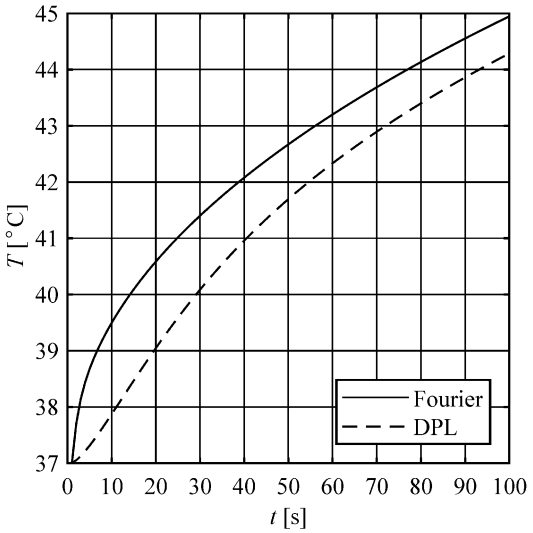

Figure 4: Course of temperature at the heated surface of biological tissue

5 CONCLUSIONS

The solution of 1D dual-phase lag equation using the general boundary element method is presented. The influence of the grid step and the number of internal cells on the accuracy of the computations is also discussed.

The examples related to the numerical modeling of thermal processes occurring in the thin metal film subjected to the ultrashort laser pulse as well as in the heated biological tissue are presented.

In future, the general boundary element method will be extended for the multilayered domains with the contact condition between the layers [11, 13, 34].

ACKNOWLEDGEMENT

Publication supported as a part of the Rector's grant in the area of research and development. Silesian University of Technology, 10/040/RGJ18/0064.

REFERENCES

[1] Tzou D. Y. *Macro- to Microscale Heat Transfer. The lagging behavior*. Taylor and Francis, (1997).
[2] Zhang Z. M. *Nano/microscale heat transfer*. McGraw-Hill, New York, (2007).
[3] Smith A. N. and Norris P. M., In: *Heat Transfer Handbook*; Adrian Bejan Ed.; John Wiley & Sons: Hoboken, 1309-1409, (2003).
[4] Chen G., Borca-Tasciuc D. and Yang R.G. In: *Encyclopedia of Nanoscience and Nanotechnology*; Hari Singh Nalwa Ed.; American Scientific Publishers: Stevenson Ranch, **7**, 429-459, (2004).
[5] Zhou J., Chen J.K. and Zhang Y. Dual phase lag effects on thermal damage to biological tissues caused by laser irradiation. *Comput. Biol. Med*. (2009) **39**: 286-293.
[6] Zhou J., Zhang Y. and Chen J.K. An axisymmetric dual-phase lag bio-heat model for laser heating of living tissues. *Int. J. Therm. Sci*. (2009) **48**, 8: 1477-1485.
[7] Liu K.Ch. and Chen H.T. Investigation for the dual phase lag behavior of bioheat transfer. *Int. J. Therm. Sci*. (2010) **49**: 1138-1146.
[8] Majchrzak E., Turchan L. and Dziatkiewicz J. Modeling of skin tissue heating using the generalized dual-phase lag equation. *ARCH MECH.* (2015) **67**, 6: 417-437.
[9] Jasiński M., Majchrzak E. and Turchan L. Numerical analysis of the interactions between laser and soft tissues using dual-phase lag model. *Appl. Math. Model.* (2016) **40**, 2: 750-762.
[10] Castro M.A., Martin J.A. and Rodriguez F. Unconditional stability of a numerical method for the dual-phase-lag equation. *Math. Probl. Eng*. (2017) 5 pages.
[11] Wang H., Dai W. and Melnik R. A finite difference method for studying thermal deformation in a double-layered thin film exposed to ultrashort pulsed lasers. *Int. Therm. Sci*.(2096) **45**, 12: 1179–1196.
[12] Majchrzak E. and Mochnacki B. Dual-phase lag equation. Stability conditions of a numerical algorithm based on the explicit scheme of the finite difference method. *J. Appl. Math. Comput. Mech*. (2016) **15**, 3: 89-96.
[13] Majchrzak E., Mochnacki B. and Suchy J.S. Numerical simulation of thermal processes proceeding in a multilayered film subjected to ultrafast laser heating. *JTAM* (2009) **47**: 383-396.
[14] Turchan L. Solving the dual-phase lag bioheat transfer equation by the generalized finite difference method. *ARCH MECH.* (2017) **69**, 4-5: 389-407.
[15] Brebbia C. A., Telles J.C.F. and Wrobel L.C. *Boundary element techniques*. Berlin, New York, Springer-Verlag, (1984).
[16] Majchrzak E. Application of different variants of the BEM in numerical modeling of bioheat transfer processes. *MCB: Mol. Cell. Biomech*. (2013) **10**, 3: 201-232.
[17] Liao S. General boundary element method for non-linear heat transfer problems governed by hyperbolic heat conduction equation. *Comput. Mech.* (1997) **20**: 397-406.

[18] Liao S. and Chwang A. General boundary element method for unsteady nonlinear heat transfer problems. *Num. Heat Tr.* (1999) **35**, 2: 225-242.
[19] Liao S.J. On the general boundary element method. *Eng. Anal. Bound. Elem*. (1998) **21**: 39-51.
[20] Hetmaniok E., Nowak I., Slota D. and Witula R. Application of the homotopy perturbation method for the solution of inverse heat conduction problem. *Int. Commun. Heat Mass* (2012) **39**: 30–35
[21] Slota D. The application of the homotopy perturbation method to one-phase inverse Stefan problem. *Int. Commun. Heat Mass* (2010) **37**: 587–592.
[22] Majchrzak E. and Mochnacki B. Numerical model of thin metal film heating using the boundary element method, *CMMS Journal* (2017) **17**, 1: 12-17.
[23] Curran D.A.S., Cross M. and Lewis B.A. Solution of parabolic differential equation by the BEM using discretization in time. *Appl. Math. Model*. (1980) **5**: 398-400.
[24] Mochnacki B. and Paruch M. Estimation of relaxation and thermalization times in microscale heat transfer model. *JTAM* (2013) **51**, 4: 837-845.
[25] Chen J.K. and Beraun J.E. Numerical study of ultrashort laser pulse interactions with metal films. *Numer. Heat Transfer. Part A* (2001) **40**: 1-20.
[26] Dai W. and Nassar R. A compact finite difference scheme for solving a one-dimensional heat transport equation at the microscale. *J.Comput. Appl. Math.* (2001) **132**: 431-441.
[27] Mitra K., Kumar S., Vedavarz A. and Moallemi M. K. Experimental evidence of hyperbolic heat conduction in processed meat. *J. Heat Tr.* (1995) **117**: 568-573.
[28] Antaki P. J. New interpretation of non-Fourier heat conduction in processed meat. *J. Heat Tr.* (2005) **127**: 189-193.
[29] Majchrzak E. and Mochnacki B. Implicit scheme of the finite difference method for 1D dual-phase lag equation. *J. Appl. Math. Comput. Mech*. (2017) **16**, 3: 37-46.
[30] Majchrzak E. and Turchan L. The general boundary element method for 3D dual-phase lag model of bioheat transfer. *Eng. Anal. Bound. Elem.* (2015) **50**: 76-82.
[31] Majchrzak E. Numerical solution of dual phase lag model of bioheat transfer using the general boundary element method. *CMES: Comput. Model. Eng. Sci*. (2010) **69**, 1: 43-60.
[32] Kumar A., Kumar S., Katiyar V.K. and Telles S. Dual phase lag bio-heat transfer during cryosurgery of lung cancer: Comparison of three heat transfer models. *J. Therm. Biol.* (2017) **69** 228-237.
[33] Mochnacki B. and Majchrzak E. Numerical model of thermal interactions between cylindrical cryoprobe and biological tissue using the dual-phase lag equation. *Int. J. Heat Mass Transf.* 108 (2017) **108**: 1-10.
[34] Karakas A., Tunc M. and Camdali U. Thermal analysis of thin multi-layer metal films during femtosecond laser heating, *Heat Mass Transfer* (2010): **46**: 1287-1293.